Eur. J. Mineral.
2009, **21**, 901–913

Flörkeite, $K_3Ca_2Na[Al_8Si_8O_{32}]\cdot 12H_2O$, a new phillipsite-type zeolite from the Bellerberg, East Eifel volcanic area, Germany

Christian L. LENGAUER[1,*], Uwe KOLITSCH[2] and Ekkehart TILLMANNS[1]

[1] Institut für Mineralogie und Kristallographie, Universität Wien, Geozentrum, Althanstrasse 14, 1090, Wien, Austria
*Corresponding author, e-mail: christian.lengauer@univie.ac.at
[2] Mineralogisch-Petrographische Abteilung, Naturhistorisches Museum, Burgring 7, 1010 Wien, Austria

Abstract: Flörkeite is a new phillipsite-type zeolite. It was found in a Ca-rich xenolith from a quarry at the Bellerberg volcano near Ettringen, East Eifel volcanic area, Germany. The paragenesis includes tobermorite, thaumasite, willhendersonite, gismondine and ellestadite. It forms subparallel, short prismatic, pseudo-monoclinic crystals elongated along [100] and flattened on {010}, with a maximum length of 0.6 mm and a thickness of up to 0.1 mm. Additional forms are {100}, {001} and {20$\bar{1}$}. Flörkeite is colourless, transparent, non-fluorescent and has a vitreous lustre and a white streak. It is brittle with irregular fracture, the calculated density is 2.266 gcm^{-3}. Optically, it is biaxial negative with $n_\alpha = 1.506(2)$, $n_\beta = 1.514(2)$, $n_\gamma = 1.518(2)$, $2V = 71.0(5)^\circ$ at 589.3 nm and 297 K. No pleochroism is observed. Orientation of the indicatrix is $X \wedge c = 43^\circ$, $Y \wedge b = 40^\circ$ and $Z \wedge a = 8^\circ$. Electron microprobe analyses yielded (wt%): Na_2O 2.32, K_2O 10.29, MgO 0.04, CaO 8.43, Al_2O_3 30.20, SiO_2 35.29, sum 86.57. A H_2O content of 15.57 wt% was derived from the single-crystal structure refinement. The empirical formula calculated on the basis of Al+Si = 16 *pfu* is $K_{2.96}Ca_{2.04}Na_{1.02}Mg_{0.01}[Al_{8.03}Si_{7.97}O_{31.97}]\cdot 11.72H_2O$ and the ideal formula can be given as $K_3Ca_2Na[Al_8Si_8O_{32}]\cdot 12H_2O$. Flörkeite is triclinic, space-group $P\bar{1}$ (no. 2), the unit-cell parameters in phillipsite-type setting are $a = 19.965(1)$, $b = 14.274(1)$, $c = 8.704(1)$ Å, $\alpha = 88.37(1)$, $\beta = 125.08(1)$, $\gamma = 89.57(1)^\circ$, $V = 2028.2(3)$ Å^3, $Z = 2$ and the $a : b : c$ ratio is 1.399 : 1 : 0.610. The five strongest lines in the powder X-ray diffraction pattern are (d in Å/I_{obs}): 3.235 / 100, 3.162 / 80, 3.135 / 80, 2.736 / 60, 4.956 / 45. The single-crystal structure refinement ($R1 = 4.39$ %) confirmed that the structure of flörkeite is the triclinically distorted analogue of phillipsite with a complete (Al,Si) ordering at the *T*-sites of the framework (mean *T*(Al)–O: 1.731–1.743 Å and *T*(Si)–O: 1.615–1.631 Å), which reduces the topochemical symmetry to $B2/b$. The K^+ cations are placed near the centre of 8-rings of the *oto* units, the Ca^{2+} and Na^+ cations are located within the *phi* units. The doubling of the *a*-parameter and the reduction of the real symmetry to $P\bar{1}$(is caused by an ordering of the extra-framework cations and H_2O molecules within the 8-ring channel system along [100], basically Ca–□–Ca, Na–Ca–Na and H_2O–K–H_2O. The (Al,Si) ordering is attributed to low-thermal genetic conditions within the Ca-rich xenolithic host, also indicated by the paragenesis with willhendersonite. Holotype material of flörkeite has been deposited at the mineral collection of the Naturhistorisches Museum Wien, Austria. The mineral is named in honour of the German mineralogist and crystallographer Otto Wilhelm Flörke (born 1926).

Key-words: flörkeite, phillipsite-(K), new mineral, zeolite, Bellerberg, Eifel, tripotassium dicalcium sodium tecto-octoalumooctosilicate dodecahydrate, (Al,Si) ordering.

1. Introduction

This paper describes and characterizes the new mineral species flörkeite, found in a xenolith from the Bellerberg volcano SE of Ettringen, Germany, which is located within the region around the Laacher See and is part of the Quaternary East Eifel volcanic area. The Bellerberg is a remnant of volcanic activity during the late Wehrer eruptive phase (Bogaard & Schmincke, 1990). It is a locality well known for uncommon and new minerals having their origin in the pyrometamorphic interaction of Ca- or Si-rich xenoliths with a leucite-tephritic lava (*e.g.*, Abraham *et al.*, 1983; Mihajlović *et al.*, 2004) and in their subsequent metasomatism (*e.g.* Lehmann, 1874) or low thermal alterations (*e.g.* Hentschel & Kuzel, 1976). The geology and mineralogy of this area were discussed and compiled by Meyer (1994) and Hentschel (1987), respectively.

According to the cited literature zeolites are often found as representatives of the late paragenetic sequence in the volcanogenic rocks of the Eifel area. At the Bellerberg, zeolites with the dense ANA and SOD framework topology (Baerlocher *et al.*, 2007) like leucite, sodalite, nosean and

0935-1221/09/0021-1952 $ 5.85
DOI: 10.1127/0935-1221/2009/0021-1952

hauyne occur in vesicles and fissures of the lava and the Si-rich xenoliths, whereas zeolites of lower framework density like levyne, thomsonite, gismondine, chabazite and phillipsite are common or accessory mineral species within the Ca-rich xenoliths. Prior to the finding of flörkeite, the Bellerberg volcano was also known as the type locality of the rare zeolites willhendersonite, $KCa[Al_3Si_3O_{12}]\cdot 5H_2O$ (Tillmanns *et al.*, 1984), bellbergite, $(K_{1.3}Sr_{0.4}Ba_{0.3})Sr_2(Ca_{3.3}Na_{0.7})Ca_2[Al_{18}Si_{18}O_{72}]\cdot 30H_2O$ (Rüdinger *et al.*, 1993) and tschörtnerite, $Ca_4(K,Ca,Sr,Ba)_3Cu_3(OH)_8[Al_{12}Si_{12}O_{48}]\cdot 14H_2O$ (Effenberger *et al.*, 1998). It is obvious from the chemical formulas that, similar to flörkeite, these zeolites exhibit (Al,Si) ordering. Up to now no structurally related compound is known for tschörtnerite. Willhendersonite and bellbergite, however, represent the (Al,Si)-ordered analogues of chabazite and synthetic zeolite TMA-E (Aiello & Barrer, 1970), respectively. This chemical conformity with flörkeite stimulated a more detailed mineralogical and structural characterization of this new zeolite and its relationship to phillipsite. Compilations of the mineralogy of phillipsite are given by Gottardi & Galli (1985) and Tschernich (1992), and a detailed crystallographical compilation of phillipsite-type compounds is given by Fischer & Baur (2006).

Flörkeite was found in a suite of xenolithic samples, collected and kindly provided to the authors as an ‘‘unusual phillipsite’’ by Bernd Ternes, Mayen – Hausen, Germany. Preliminary results on the structural characteristics of the new mineral were given by Kolitsch & Blass (2005). The mineral is named in honour of the German mineralogist and crystallographer Otto Wilhelm Flörke (born 1926), his leading contributions to microstructure, crystal-chemistry and structural state of the silica polymorphs (*e.g.*, Flörke, 1967; Flörke *et al.*, 1984) and his leisure-time interests in the mineralogy of the Eifel region. The similar sounding and discredited zeolite from Iceland, flokite, was proven by Davis (1958) to be identical to mordenite.

Prior to publication, mineral species status, and name of flörkeite have been approved by the International Mineralogical Association Commission on New Minerals, Nomenclature and Classification (IMA 2008-036). The investigated holotype material is preserved at the mineral collection of the Naturhistorisches Museum Wien (NHMW), Austria, with catalogue number 2009-IV-a.

2. Occurrence and paragenesis

The investigated material was found in the quarry of the firm ‘A. Caspar’ within the Bellerberg volcano (N 50° 21′ 9″ E 7° 14′ 3″). Similar to the previous findings of zeolites, flörkeite occurs in small cavities of a pyrometamorphically modified Ca-rich xenolith of the Tertiary basement, which was enclosed with the leucite-tephritic lava. The vesicles of the type material are predominantly filled or coated with white, spherolitic intergrown masses of tobermorite, which is partially covered by a thin layer of thaumasite. Within the modified limestone, blue hauyne and wollastonite can be observed. Flörkeite has crystallized on tobermorite, thus representing the last, low-thermal alteration product of the xenolith. A further final phase of the crystallization sequence found in this paragenesis is willhendersonite, which occurs as clear platelets, flattened on {001} and grown on gismondine. Additionally, ettringite, portlandite, strätlingite, thomsonite, cuspidine and reinhardbraunsite are known from such similar parageneses (Hentschel, 1987).

3. Appearance and physical properties

The flörkeite-type material consists of subparallel, short prismatic, pseudo-monoclinic crystals (Fig. 1a and b) elongated along [100] and flattened on {010}, with a maximum length of 0.6 mm and a thickness of up to 0.1 mm. The additional dominant form is {001} and subordinate {100}. If the $\{20\bar{1}\}$ form is more predominant a short pseudo-columnar habit evolves, which is characteristic for Morvenite-twinned (pseudo-tetragonal) phillipsites (Tschernich, 1992), rarely observed in the Eifel area (Hentschel, 1987). For flörkeite, however, twinning is not observed. The mineral is colourless, transparent, non-fluorescent and has vitreous lustre and a white streak. Tenacity is brittle with irregular fracture; no parting and an indistinct cleavage on {001} is observed. The Mohs hardness was not determined, the calculated density based on the empirical chemical formula is 2.266 gcm^{-3}, and 2.270 gcm^{-3} on the single-crystal structure refinement.

Flörkeite fragments were mounted on glass fibres and inspected under a polarizing microscope equipped with a spindle stage. Optical angle and orientation of the optical axis were determined with the software EXCALIBR II (Bartelmehs *et al.*, 1992). The mineral is biaxial negative with $n_\alpha = 1.506(2)$, $n_\beta = 1.514(2)$, $n_\gamma = 1.518(2)$, $2V_{obs} = 71.0(5)^\circ$ ($2V_{calc} = 70.2^\circ$) at 589.3 nm and 297 K. The orientation of the indicatrix is $X \wedge c = 43^\circ$, $Y \wedge b = 40^\circ$ and $Z \wedge a = 8^\circ$. The dispersion is weak ($r < v$) and no pleochroism is observed. The calculation of the compatibility index (Mandarino, 1981) based on the empirical values of the oxide and the calculated H_2O content revealed 0.022, which is classified as excellent. In comparison to the optical data given by Galli & Loschi Ghittoni (1972) for phillipsite, flörkeite exhibits higher refractive index values, which can be mainly attributed to the higher content of charge-balancing extra-framework cations.

4. Chemical composition

The results of the chemical analyses of flörkeite, the used standard materials, the measurement conditions as well as

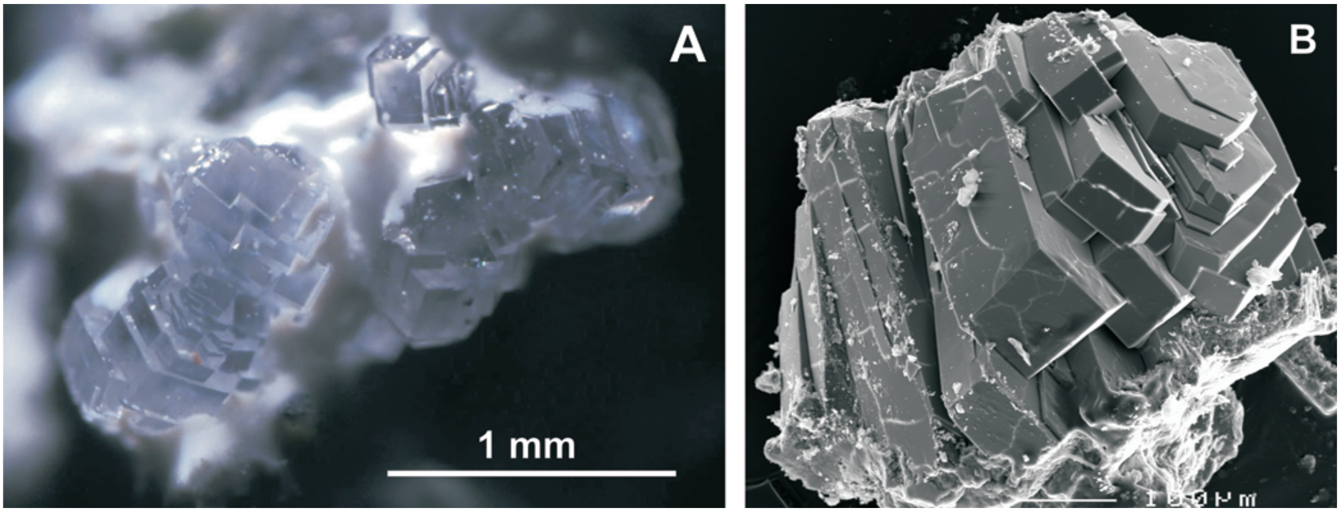

Fig. 1. Microphotograph (a) of flörkeite from the Bellerberg, Eifel, Germany, and a back-scattered electron image (b) of an aggregate of intergrown flörkeite crystals showing the predominant tabular habit, flattened on {010}, and irregular fissures at the surface due to dehydration under the evacuating conditions of the electron microscope. Aggregate diameter is about 0.5 mm. Microphotography by courtesy of E. van der Meersche, Gent.

the reported ranges of the constituents for phillipsite are listed in Table 1. The mean value of the sums of the oxides is 86.57 wt% (range: 84.39–88.84 wt%), which would equate to a H_2O content ~10 H_2O *pfu*, a value significantly below the reported H_2O range for phillipsite (Table 1). Due to the scarce amount of available material, a direct measurement of the H_2O content by means of thermal analysis was not possible. Additionally, the vacuum conditions within the electron microprobe known to initiate at least partial dehydration of zeolite-type materials have to be taken into account. The single-crystal structure refinement, on the other hand, revealed a content of 12 H_2O molecules within the unit-cell, which is equivalent to 15.57 wt% H_2O. Therefore, this value was selected as the empirical H_2O-content of the flörkeite composition (Table 1).

Using the general structural formula of phillipsite-type compounds $(M^{1+},M^{2+}{}_{0.5})_x[Al_xSi_{16-x}O_{32}] \cdot yH_2O$ (Coombs *et al.*, 1998) the empirical formula calculated on the basis of Al+Si = 16 *pfu* can be given as $K_{2.96}Ca_{2.04}Na_{1.02}Mg_{0.01}[Al_{8.03}Si_{7.97}O_{31.97}]\cdot 11.72H_2O$, which is very close to the ideal formula $K_3Ca_2Na[Al_8Si_8O_{32}]\cdot 12H_2O$. Besides MgO (0.04 wt%, range: 0.00–0.12 wt%) no other elements with an atomic number greater than 8, *e.g.* Sr and Ba, were detected. Comparing these results to the ranges reported for phillipsite (Table 1) the flörkeite chemistry is outstanding by an almost perfect Al:Si ratio of 1:1 based on increased Al_2O_3 and reduced SiO_2 values, which deviate by about ±5 wt% from the values given for high Al-bearing phillipsites, $K_2Ca_2Na_{0.5}[Al_{6.5}Si_{9.5}O_{32}]\cdot 14H_2O$, by Galli & Loschi

Table 1. Electron microprobe analyses of flörkeite (wt%).

Constituent	Mean[a]	Range	S.D.	Calc.[b]	Standard	Phillipsite[c]
Na_2O	2.32	1.96–2.53	0.27	2.23	albite	0.00–9.80
K_2O	10.29	9.74–10.41	0.18	10.17	orthoclase	2.38–13.00
MgO	0.04	0.00–0.12	0.06		olivine	0.00–6.41
CaO	8.43	8.01–9.17	0.21	8.07	wollastonite	0.00–10.14
Al_2O_3	30.20	29.36–30.98	0.42	29.36	corundum syn.	16.24–25.98
SiO_2	35.29	34.16–36.02	0.68	34.60	quartz syn.	41.42–55.23
Sum	86.57	84.39–88.84	1.45	84.43		
H_2O	15.57_{calc}			15.57		15.06–17.88
Total	102.14			100.00		

Measurement conditions: Cameca SX100 instrument, wavelength-dispersive mode, 15 kV, 15 nA sample current, beam diameter ~5 µm, counting time 20 s per element.
[a] 11 measurements of 4 fragments.
[b] Calculated required chemical composition of the end-member $K_3Ca_2Na[Al_8Si_8O_{32}]\cdot 12H_2O$.
[c] Chemical ranges according to the compilations of Doelter (1921) and Galli & Loschi Ghittoni (1972).

Ghittoni (1972). Consequently, the overall sum of the charge-balancing cation oxides (∼21 wt%) is significantly higher. With regard to the K-dominance of these cations, however, flörkeite is in conformity with the variability of the alkaline and earth-alkaline constituents, see *e.g.* the compilation of Doelter (1921) for phillipsite-(K) from Capo di Bove (#20–22) and Vallerano (#23). Also taking into account the K:Ca:Na ratio, flörkeite matches with the field of phillipsite chemistry (#9 and 17 of Galli & Loschi Ghittoni, 1972).

Table 2. X-ray powder diffraction data for flörkeite.

I_obs	d_obs	$I_\text{calc}{}^\text{a,b}$	$d_\text{calc}{}^\text{a}$	*h*	*k*	*l*
<5	14.310	3.9	14.2622	0	1	0
<5	8.623	2.4	8.5770	1	0	−1
5	8.185	2.9	8.1799	2	0	−1
		1.6	8.1661	2	0	0
20	7.132	19.0	7.1311	0	2	0
		11.7	7.1176	0	0	1
10	6.506	6.0	6.4729	0	1	1
		4.5	6.4666	1	−2	0
5	6.254	13.4	6.2691	0	1	−1
20	5.417	25.0	5.4206	2	−2	−1
		3.5	5.3967	1	2	−1
15	5.289	18.7	5.2955	2	−2	0
45	4.965	32.5	4.9911	4	0	−1
		25.0	4.9398	0	2	−1
20	4.287	18.1	4.2885	2	0	−2
		5.0	4.2825	2	0	1
15	4.145	17.0	4.1468	2	1	1
		6.2	4.1407	2	−3	−1
35	4.065	16.6	4.0747	4	−2	−1
		17.9	4.0579	2	−1	1
<5	3.957	2.8	3.9560	4	1	0
5	3.889	5.1	3.8955	4	−1	0
		3.2	3.8822	0	−3	1
5	3.497	5.1	3.4997	4	−2	0
		2.6	3.4858	0	1	2
10	3.424	4.2	3.4295	4	−3	−1
		4.4	3.4209	0	−1	2
35	3.300	23.5	3.3031	2	4	0
		6.5	3.2889	2	−4	−1
100	3.235	10.9	3.2414	6	0	−2
		28.5	3.2403	0	4	1
		7.5	3.2388	6	0	−1
		6.7	3.2378	2	−3	−2
		24.1	3.2365	0	2	2
		22.3	3.2333	2	−4	0
80	3.162	25.6	3.1620	6	−1	−2
		13.8	3.1595	6	1	−2
80	3.135	25.9	3.1380	0	4	−1
		19.8	3.1345	0	2	−2
5	3.076	1.3	3.0775	1	1	2
		1.8	3.0750	4	3	−2
25	2.966	15.6	2.9673	6	2	−1
10	2.933	6.9	2.9308	6	−2	−1
10	2.896	10.8	2.9001	4	0	−3
		5.6	2.8952	4	0	1
20	2.790	6.0	2.7958	0	−3	2
		7.5	2.7872	2	−4	−2
60	2.736	9.6	2.7391	2	0	−3
		17.7	2.7366	2	0	2
40	2.712	13.7	2.7176	2	5	0
40	2.665	9.2	2.6603	4	2	−3
		2.2	2.6596	6	−1	0
20	2.572	10.1	2.5708	0	4	2
10	2.520	2.0	2.5209	2	−2	2
		2.5	2.5187	6	−2	0
10	2.456	4.2	2.4614	8	1	−2
		4.1	2.4551	8	−1	−2
5	2.415	4.0	2.4144	2	3	2
		1.8	2.4120	2	−5	−2
15	2.372	6.4	2.3710	4	5	0
10	2.357	2.5	2.3583	4	−5	−2
		1.9	2.3563	8	0	−3
5	2.322	3.7	2.3225	8	1	−3
		1.4	2.3214	4	5	−2
5	2.282	2.4	2.2822	0	6	1
5	2.210	2.4	2.2114	2	−4	−3
10	2.184	3.4	2.1837	6	−4	−3
		4.7	2.1835	0	5	−2
15	2.041	5.8	2.0415	8	0	0
		1.3	2.0403	4	6	−2
25	1.977	4.8	1.9780	8	2	0
		5.3	1.9766	10	0	−2
5	1.941	2.0	1.9419	6	−3	1
		1.6	1.9388	2	−2	−4
5	1.861	5.5	1.8610	0	5	3
		1.0	1.8564	8	−3	0
5	1.829	1.8	1.8317	2	6	2
		1.3	1.8286	2	−6	−3
25	1.783	8.5	1.7828	0	8	0
10	1.760	4.2	1.7612	8	4	−4
		2.3	1.7596	2	−6	2
5	1.746	1.2	1.7462	6	−5	−4
		1.1	1.7459	0	8	1
10	1.714	2.8	1.7148	8	−6	−2

Measurement conditions: camera Ø 114.59 mm, Cu$K\alpha$, Ni-filtered, 24 h; I_obs estimated visually.

[a] d_calc, I_calc and *hkl* assignment based on a theoretical powder pattern calculated with PC-Rietveld Plus (Fischer *et al.*, 1993) using the cell and structural parameters of the single-crystal structure refinement.

[b] I_calc is normalized to $\Sigma I_\text{calc} = 100$ of the 6 overlapping intensities at $d_\text{obs} = 3.235$ Å.

5. X-ray diffractometry

The observed powder X-ray diffraction (PXRD) data for flörkeite (Table 2) were obtained with a Debye-Scherrer camera equipped with a Gandolfi attachment (Gandolfi, 1964) in asymmetric setting (Straumanis & Jevinš, 1936) to correct the d_obs data for film shrinkage. The calculated PXRD pattern of flörkeite and for comparative purposes the measured PXRD pattern of a phillipsite from Sasbach, Germany, are shown in Fig. 2. The overall outlines of both PXRD patterns are similar. For identification purposes the most significant difference between the PXRD patterns, also clearly evident on the film exposure of flörkeite, is the

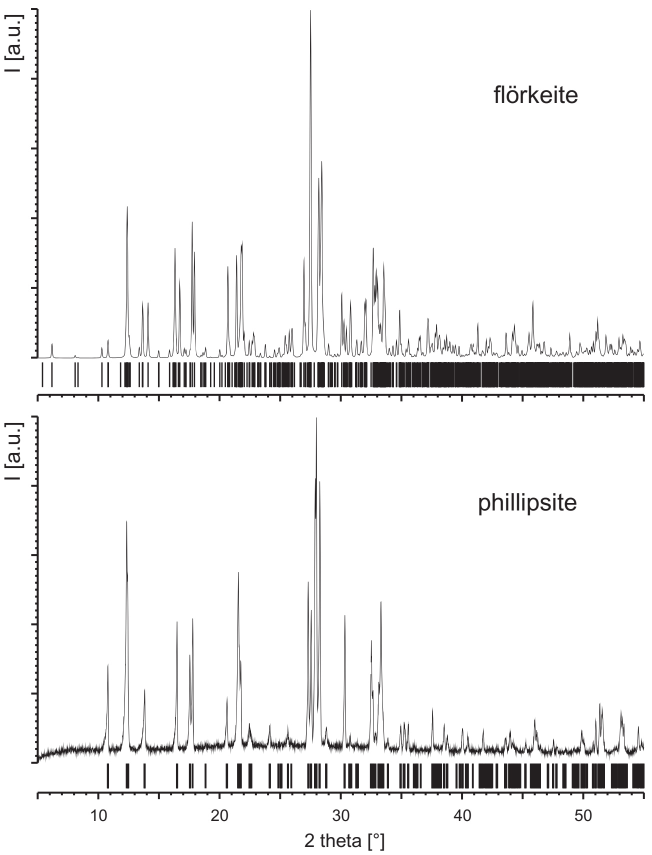

Fig. 2. Calculated PXRD pattern of flörkeite (upper curve) based on the positional and isotropic displacement parameters of the single-crystal refinement assuming Cu$K\alpha1$ radiation in comparison to an observed pattern of phillipsite (lower curve). For both the calculated peak positions are given as vertical tick marks below the patterns. Phillipsite sample: Sasbach, Germany (Institut für Mineralogie und Kristallographie, Universität Wien, collection no. 3929, year 1871), $(Ca_{1.4}K_{1.3}Na_{0.4})[Al_{4.7}Si_{11.3}O_{32}] \cdot 13.3H_2O$ (Fresenius, 1879); capillary measurement: Cu$K\alpha1$, X'PertMPD; refined unit-cell parameters: a = 9.963(1), b = 14.220(2), c = 8.731(1) Å, β = 124.94(1)°, PC-Rietveld Plus (Fischer *et al.*, 1993).

occurrence of split reflections at ~13.8 and ~16.5 °2θ, *i.e.* d_{obs} 6.506/6.254 Å and 5.417/5.289 Å (Table 2). In the low angular region only one weak reflection at ~10.2 °2θ (d_{obs} 8.623 Å) is indicative for the doubling of the a parameter. Also peak splitting, which would be a prove for the lowering of the unit-cell symmetry, is below the angular resolution of the film method. Consequently, the verification of real symmetry and cell metric as well as the reliable refinement of the unit-cell parameters of flörkeite are prevented on the basis of the low resolution film data. Therefore, the unit-cell parameter values and the real symmetry obtained from the single-crystal work (Table 3) are taken for the further description of flörkeite.

The unit-cell parameters of flörkeite in the phillipsite-type cell setting are a = 19.965(1), b = 14.274(1), c = 8.704(1) Å, α = 88.37(1), β = 125.08(1), γ = 89.57(1)° and the $a : b : c$ ratio is 1.399 : 1 : 0.610. The values of the reduced cell are a = 8.704(1), b = 14.274(1), c = 16.572(1) Å, α = 91.37(1), β = 99.62(1), γ = 91.63(1)°, the corresponding transformation matrix (phi → red) is $\mathbf{a}, -\mathbf{b}, \mathbf{a}+\mathbf{c}$. In comparison to phillipsite-(K) (Rinaldi *et al.*, 1974: a = 9.865, b = 14.300, c = 8.668 Å, β = 124.20°), it is apparent that flörkeite exhibit a pseudomonoclinic, triclinically distorted unit-cell metric ($\Delta_\alpha = 1.63(1)$, $\Delta_\gamma = 0.43(1)°$) accompanied by an almost perfect doubling of the a parameter ($a_{\text{flö}} = 2.024 \times a_{\text{phi}}$). Figure 3 gives a schematic representation of the unit-cell relationships between flörkeite, phillipsite and the orthorhombic PHI-aristotype.

The single-crystal intensity data for flörkeite were collected on a Nonius KappaCCD diffractometer. For data collection, reduction, processing and absorption correction by the multi-scan approach the HKL/HKL-2000 software package (Otwinowski & Minor, 1997; Otwinowski *et al.*, 2003) was used. For the structure solution and refinement the SHELX-97 software (Sheldrick, 1997a and b) was applied. For collecting the data the whole Ewald sphere up to 30.51 °θ was covered by a measurement strategy, which resulted in a three-fold overall redundancy of the recorded reflections. After integrating and scaling the total of 55455 (53145 with $I > 1$) reflections in space-group $P\bar{1}$ the evaluation of the Friedel-pair intensity statistics revealed space-group $P\bar{1}$. Subsequently, the reflections were reduced to a unique dataset of 12360 reflections (R_{int} 2.07 %) and 10386 reflections with $F_o^2 > 2\sigma(F_o^2)$ by the refinement software; six inconsistent equivalents were recorded during the data processing. The doubling of the a-parameter was proven by evaluating the phillipsite-type, odd h00 reflections, which despite the fact of exhibiting relative intensities ~1%, resulted in significant intensities with a mean $F_o^2/\sigma(F_o^2)$ of 27.0 in comparison to 37.8 for the even reflections. Further details of the data collection, the structure refinement and other relevant crystallographic data for flörkeite are summarized in Table 3.

The structure of flörkeite was solved using direct methods, which revealed 6 extra-framework and 48 framework sites. Subsequent difference Fourier maps helped to work out the atom occupancy at the extra-framework sites as well as 12 oxygen positions suitable to be interpreted as H_2O molecules; the Al-and Si-allocation of the tetrahedrally coordinated framework sites (T-sites) was done on the basis of the interatomic T–O distances. During the steps of structure solution and refinement the reduced setting of the data collection was transformed to the phillipsite-type cell applying the HKLF 3 × 3 matrix command extension. The refinement of the structural parameters using complex neutral scattering factors (Wilson & Prince, 1999) was started with isotropic displacement parameters. During the occupancy refinement in the extra-framework sites, all occupancy values did not significantly deviate from 1, except for one K-position ($\text{occ.}_{K3} = 0.923(3)$). Finally, for all framework and extra-framework sites anisotropic displacement values were added as variable parameters. The refinement converged at $R1$ = 4.39 % (w$R2$ = 10.86 %) and the maximum peaks in the final difference-Fourier map were −0.78 and 1.36 eÅ^{-3}. Based on this single-crystal work the not charge-balanced formula can be

Table 3. Single-crystal X-ray data collection and structure refinement of flörkeite.

Space-group	$P\bar{1}$, no. 2		θ range (°)	3.08–30.51
	phi[a]	red[a]	h, k, l ranges	$-28 < h < 28$
a (Å)	19.965(1)	8.704(1)		$-20 < k < 20$
b (Å)	14.274(1)	14.274(1)		$-12 < l < 12$
c (Å)	8.704(1)	16.572(1)	No. of total reflections	55455
α (°)	88.37(1)	91.37(1)	No. of unique F_o^2 (n)	12360 (R_{int} 2.07 %)
β (°)	125.08(1)	99.62(1)	No. of $F^2_o > 2\sigma$ (F_o^2)	10386
γ (°)	89.57(1)	91.63(1)	No. of parameters (p)	596
V (Å^3)	2028.2(3)		$R1$, $R1 > 2\sigma$ (F_o^2)	4.39, 3.53 %
Z	2		w$R2$, w$R2 > 2\sigma$ (F_o^2)	10.86, 10.31 %
Formula weight	2772.93		GOF, Δ_{max}/σ	1.040, 0.001
D (gcm^{-3})	2.270		Δ eÅ$^{-3}_{\text{min, max}}$	−0.78, 1.36
Wavelength (Å)	0.71073		Crystal size (mm)	0.13 × 0.17 × 0.18
μ Mo$K\alpha$ (cm^{-1})	1.137		Transmission factors	0.822–0.866
			Absorption correction	Multi-scan

$R1 = \Sigma\,(||F_o|-|F_c||)/\Sigma\,|F_o|$, w$R2 = [\Sigma\,\mathrm{w}(F_o{}^2-F_c{}^2)^2/\Sigma\,\mathrm{w}(F_o{}^2)^2]^{1/2}$,

$R_{int} = \Sigma|F_o{}^2-F_o{}^2(\mathrm{mean})|/\Sigma\,F_o{}^2$, GOF $= \{\Sigma[\mathrm{w}(F_o{}^2-F_c{}^2)^2]/(n-p)\}^{1/2}$,

$\mathrm{w} = 1/[\sigma^2 F_o{}^2+(0.056 \times \mathrm{P})^2 + 2.506 \times \mathrm{P}]$, $\mathrm{P} = [\max(F_o{}^2,0) + 2 \times F_c{}^2]/3$.

Measurement conditions: Nonius four-circle KappaCCD diffractometer, primary graphite monochromator, 0.3 mm capillary-optics collimator. Data were collected using one φ-scan and six sets of ω-scans with a total of 440 frames of 2° rotation width, 2 × 90 s exposure time/frame, crystal-detector distance of 45 mm.

[a] The transformation from the reduced cell setting of the data collection (red) to the phillipsite-type (phi) setting is −**a** + **c**, −**b**, **a**.

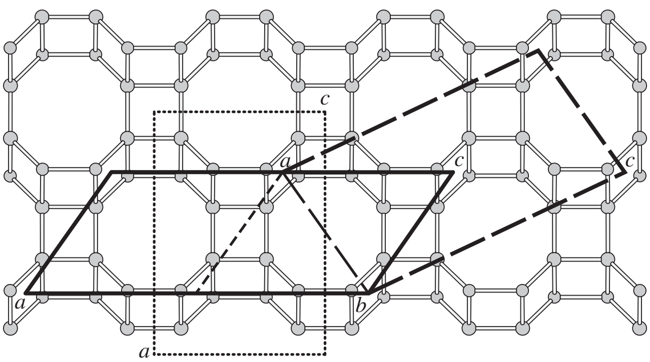

Fig. 3. Schematic representation, modified and extended after Fischer & Baur (2006), along [010] of the relationships between the pseudo-monoclinic phillipsite-type (bold solid line) and reduced cell (bold dashed line) of flörkeite, phillipsite (dashed line at *a*/2) and the orthorhombic cell (spacegroup: *Bmmb*, origin shift: −¼, 0, ¼) of the PHI-aristotype (dotted line), all projected on the aristotype *T*-site (gray) arrangement at *y* ± 0.15.

given as $K_{2.93}Ca_2Na\ [Al_8Si_8O_{32}]\cdot 12H_2O$, which agrees well with the results of the chemical analyses. For the labelling of the framework sites the atomic site relationship of Baur & Fischer (2000) was applied by transforming the standardized PHI-II.2 type coordinates to the PHI-VIII.2 type of flörkeite (pers. comm. R.X. Fischer). The final positional coordinates, the equivalent isotropic displacement parameters and the site occupancy values, as well as the interatomic distances to the equivalent sites of phillipsite-(K) (Rinaldi *et al.*, 1974) are given in Table 4. For the extra-framework sites of flörkeite the structurally equivalent cations and H_2O molecules of phillipsite-(K) are additionally denoted for the crystallographic sites. In Table 5 selected bond distances and angles for the framework sites, in Table 6 the distances for the extra-framework cation sites and in Table 7 the closest O–O distances for the H_2O molecules are given.

6. Structural description and discussion

6.1. Framework features

The main feature of phillipsite-type framework structures, IZA-code PHI (Baerlocher *et al.*, 2007), is an almost orthogonal cross-linked system of double-connected 4-ring chains, a double crankshaft chain (*cc*) along [100] and a sinusoidal chain (*cf.* Gottardi & Galli, 1985: Fig. 0.2 L c) parallel (40$\bar{1}$). Both chains establish an interconnected channel system of alternating *phi* ($4^4 4^2 4^1 8^2 8^2 8^1$) and *oto* ($4^2 4^2 4^1 8^2 8^1$) units (Smith, 2000) along the **a** (*kfe* channel) and **b** vector (*kgu* channel) (Figs. 4a and 5a), both with an ideally circular 8^2-ring opening (Fischer & Baur, 2006). Along the **c** vector a further trapezoid-shaped 8-ring channel system exists. The *kfe* channels are linked *via* connecting sheets of *T*-sites parallel (010), which are shown in the framework presentations in Figs. 3 and 4. Due to the almost orthogonal build-up of the double-connected 4-ring chains a pseudo-orthorhombic symmetry is evident for all PHI-type compounds. Therefore, the highest possible topological symmetry of the PHI-aristotype (Fig. 3) is orthorhombic with space-group *Bmmb*. In the structure of phillipsite this *T*-site arrangement is monoclinically

Table 4. Structural parameters for flörkeite, standard deviations in parentheses.

Tetrahedrally coordinated framework sites

Site[a]		Atom	x	y	z	U_{equiv}[b]	Δ_{Rin74}[c]
*T*11a1	[2(i), 1]	Al	0.02844(3)	0.49169(4)	0.28751(8)	0.0080(1)	0.056
*T*11a2	[2(i), 1]	Al	0.52883(3)	0.49306(4)	0.28907(8)	0.0098(1)	0.062
*T*11b1	[2(i), 1]	Al	0.87079(3)	0.02570(4)	0.26861(8)	0.0075(1)	0.142
*T*11b2	[2(i), 1]	Al	0.37495(3)	0.03013(4)	0.27589(8)	0.0087(1)	0.180
*T*12a1	[2(i), 1]	Si	0.37201(3)	0.46214(4)	0.29001(7)	0.0093(1)	0.198
*T*12a2	[2(i), 1]	Si	0.87106(3)	0.46418(4)	0.28681(7)	0.0087(1)	0.164
*T*12b1	[2(i), 1]	Si	0.53421(3)	0.00003(4)	0.28286(7)	0.0107(1)	0.142
*T*12b2	[2(i), 1]	Si	0.03764(3)	−0.00150(3)	0.29276(7)	0.0077(1)	0.178
*T*21a1	[2(i), 1]	Si	0.43055(3)	0.64274(4)	0.93572(7)	0.0099(1)	0.178
*T*21a2	[2(i), 1]	Si	0.92821(3)	0.64052(3)	0.92854(7)	0.0087(1)	0.225
*T*21b1	[2(i), 1]	Si	0.79195(3)	0.85668(3)	0.01889(7)	0.0078(1)	0.162
*T*21b2	[2(i), 1]	Si	0.29368(3)	0.85804(3)	0.03109(7)	0.0084(1)	0.250
*T*22a1	[2(i), 1]	Al	0.29112(3)	0.64051(4)	0.99642(8)	0.0089(1)	0.039
*T*22a2	[2(i), 1]	Al	0.78790(3)	0.63934(4)	0.98581(8)	0.0090(1)	0.095
*T*22b1	[2(i), 1]	Al	0.93495(3)	0.86340(4)	0.95613(8)	0.0080(1)	0.098
*T*22b2	[2(i), 1]	Al	0.43047(3)	0.86598(4)	0.94411(8)	0.0090(1)	0.170

Oxygen framework sites

Site[a]		Atom	x	y	z	U_{equiv}[b]	Δ_{Rin74}[c]
O11a1	[2(i), 1]	O	0.32887(9)	0.5601(1)	0.1795(2)	0.0191(3)	0.300
O11a2	[2(i), 1]	O	0.82589(8)	0.5612(1)	0.1755(2)	0.0182(3)	0.274
O11b1	[2(i), 1]	O	0.51464(9)	0.9138(1)	0.1437(2)	0.0150(3)	0.082
O11b2	[2(i), 1]	O	0.01834(9)	0.9097(1)	0.1620(2)	0.0138(3)	0.129
O12a1	[2(i), 1]	O	−0.00618(8)	0.5851(1)	0.1255(2)	0.0178(3)	0.308
O12a2	[2(i), 1]	O	0.49271(9)	0.5879(1)	0.1336(2)	0.0219(3)	0.342
O12b1	[2(i), 1]	O	0.82500(9)	0.9166(1)	0.2062(2)	0.0141(3)	0.165
O12b2	[2(i), 1]	O	0.33359(9)	0.9193(1)	0.2178(2)	0.0148(3)	0.232
O21a1	[2(i), 1]	O	0.31560(8)	0.3733(1)	0.1849(2)	0.0151(3)	0.259
O21a2	[2(i), 1]	O	0.81019(8)	0.3759(1)	0.1938(2)	0.0121(2)	0.214
O21b1	[2(i), 1]	O	0.58569(9)	0.0802(1)	0.2576(2)	0.0149(3)	0.392
O21b2	[2(i), 1]	O	0.07803(8)	0.0826(1)	0.2434(2)	0.0123(3)	0.279
O22a1	[2(i), 1]	O	0.07289(9)	0.4007(1)	0.2443(2)	0.0174(3)	0.120
O22a2	[2(i), 1]	O	0.56709(9)	0.4014(1)	0.2306(2)	0.0181(3)	0.018
O22b1	[2(i), 1]	O	0.80339(8)	0.1142(1)	0.1153(2)	0.0146(3)	0.483
O22b2	[2(i), 1]	O	0.30379(9)	0.1181(1)	0.1362(2)	0.0186(3)	0.312
O31a	[2(i), 1]	O	0.54043(9)	0.2499(1)	0.0415(2)	0.0180(3)	0.160
O31b	[2(i), 1]	O	0.04227(8)	0.2528(1)	0.0452(2)	0.0181(3)	0.195
O32a	[2(i), 1]	O	0.19655(9)	0.2519(1)	0.9143(2)	0.0157(3)	0.219
O32b	[2(i), 1]	O	0.69751(9)	0.2513(1)	0.9050(2)	0.0146(3)	0.247
O41a	[2(i), 1]	O	0.45767(9)	0.4419(1)	0.3144(2)	0.0179(3)	0.361
O41b	[2(i), 1]	O	0.95249(9)	0.4418(1)	0.2966(2)	0.0159(3)	0.268
O42a	[2(i), 1]	O	0.95757(8)	0.0391(1)	0.2729(2)	0.0143(3)	0.199
O42b	[2(i), 1]	O	0.45140(9)	0.0468(1)	0.2427(2)	0.0189(3)	0.298
O51a	[2(i), 1]	O	0.33584(9)	0.6396(1)	0.8706(2)	0.0161(3)	0.404
O51b	[2(i), 1]	O	0.83552(9)	0.6349(1)	0.8697(2)	0.0186(3)	0.386
O52a	[2(i), 1]	O	0.84355(9)	0.8837(1)	0.9338(2)	0.0162(3)	0.236
O52b	[2(i), 1]	O	0.33933(9)	0.8775(1)	0.9277(2)	0.0154(3)	0.231
O61a	[2(i), 1]	O	0.38921(9)	0.4655(1)	0.4974(2)	0.0146(3)	0.218
O61b	[2(i), 1]	O	0.89235(8)	0.4634(1)	0.4981(2)	0.0126(3)	0.232
O62a	[2(i), 1]	O	0.40581(9)	0.0463(1)	0.5041(2)	0.0178(3)	0.431
O62b	[2(i), 1]	O	0.88963(8)	0.0335(1)	0.4905(2)	0.0130(3)	0.195

Extra-framework sites

Site[a]	Atom	Occ.[d]	x	y	z	U_{equiv}[b]	Δ_{Rin74}[c]
K1	K	1	0.42233(4)	0.25788(4)	0.1458(1)	0.0364(1)	0.53/K
K2	K	1	0.93846(4)	0.25093(4)	0.2404(1)	0.0391(2)	0.27/K
K3	K	0.929(3)	0.58471(4)	0.74160(5)	0.3841(1)	0.0401(2)	0.58/W2
Ca1	Ca	1	0.79023(2)	0.34993(3)	0.45758(6)	0.01545(8)	1.57/W4
Ca2	Ca	1	0.80461(3)	0.87723(3)	0.44598(6)	0.01831(9)	0.07/Ca
Na1	Na	1	0.29777(6)	0.86755(8)	0.4346(1)	0.0286(2)	0.14/Ca

Table 4. Continued

Site[a]	Atom	Occ.[d]	Extra-framework sites x	y	z	U_{equiv}[b]	Δ_{Rin74}[c]
OW1	O	1	0.8871(1)	0.7439(1)	0.4771(3)	0.0297(4)	0.19/W1
OW2	O	1	0.0646(1)	0.7391(1)	0.4181(3)	0.0408(5)	0.27/W2
OW3A	O	1	0.1543(1)	0.8573(2)	0.1475(3)	0.0344(4)	0.20/W3
OW3B	O	1	0.6626(1)	0.8808(1)	0.1736(2)	0.0274(4)	0.41/W3
OW3C	O	1	0.1391(1)	0.6690(2)	0.2085(3)	0.0478(6)	0.72/W3
OW3D	O	1	0.6850(3)	0.6313(2)	0.2069(5)	0.093(1)	0.46/W3
OW4A	O	1	0.2503(1)	0.2550(2)	0.4746(3)	0.0389(5)	0.38/W4
OW4B	O	1	0.7734(1)	0.1803(1)	0.4227(2)	0.0218(3)	1.10/W4
OW5A	O	1	0.2488(1)	0.5004(1)	0.4791(3)	0.0337(4)	0.17/W5
OW5B	O	1	0.2520(1)	0.0352(1)	0.4237(2)	0.0260(4)	–
OW6	O	1	0.5291(2)	0.2673(2)	0.5426(4)	0.0582(7)	–
OW7	O	1	0.3105(1)	0.6972(1)	0.4630(2)	0.0265(4)	1.03/Ca

[a] Labelling of the framework sites according to the enumeration scheme of Baur & Fischer (2000), Wyckoff positions and site symmetries in square brackets. The extra-framework sites are partially designated after Rinaldi *et al.* (1974).
[b] The equivalent isotropic displacement factor as defined by Fischer & Tillmanns (1988).
[c] Distance (Å) to the equivalent site in phillipsite-(K) of Rinaldi *et al.* (1974).
[d] Site occupancy values.

Table 5. Selected interatomic distances (Å) and angles (°) for the framework sites in flörkeite, standard deviations in parentheses.

		Al–O			Si–O	Si–O–Al			Al–O			Si–O	Si–O–Al
*T*11a1	– O41b	1.722(2)	*T*12a1	– O11a1	1.604(2)	154.2(1)	*T*22a1	– O11a1	1.711(2)	*T*21a1	– O12a2	1.604(2)	155.0(1)
	– O12a1	1.733(2)		– O21a1	1.618(2)	134.0(1)		– O32b	1.741(2)		– O31a	1.620(2)	144.9(1)
	– O22a1	1.735(2)		– O41a	1.620(2)	143.0(1)		– O21a2	1.751(2)		– O22a2	1.620(2)	144.9(1)
	– O61b	1.757(2)		– O61a	1.634(2)	132.1(1)		– O51a	1.767(2)		– O51a	1.634(2)	132.9(1)
Mean		1.737			1.619	140.8			1.743			1.620	144.4
*T*11a2	– O12a2	1.715(2)	*T*12a2	– O11a2	1.603(2)	151.6(1)	*T*22a2	– O11a2	1.729(2)	*T*21a2	– O31b	1.612(2)	147.3(1)
	– O41a	1.722(2)		– O41b	1.608(2)	144.0(1)		– O21a1	1.733(2)		– O12a1	1.615(2)	154.3(1)
	– O22a2	1.739(2)		– O61b	1.632(1)	134.4(1)		– O32a	1.742(2)		– O51b	1.615(2)	136.1(1)
	– O61a	1.751(2)		– O21a2	1.634(1)	136.7(1)		– O51b	1.743(2)		– O22a1	1.619(2)	139.4(1)
Mean		1.732			1.619	141.7			1.737			1.615	144.3
*T*11b1	– O42a	1.724(2)	*T*12b1	– O42b	1.615(2)	143.3(1)	*T*22b1	– O31b	1.718(2)	*T*21b1	– O32a	1.608(2)	137.4(1)
	– O22b1	1.733(2)		– O62a	1.636(2)	141.6(1)		– O52a	1.741(2)		– O22b2	1.613(2)	145.4(1)
	– O12b1	1.748(2)		– O21b1	1.636(2)	130.9(1)		– O11b2	1.754(2)		– O52a	1.620(2)	144.5(1)
	– O62b	1.750(2)		– O11b1	1.638(2)	138.7(1)		– O21b2	1.755(2)		– O12b1	1.636(1)	130.5(1)
Mean		1.739			1.631	138.6			1.742			1.619	139.5
*T*11b2	– O22b2	1.725(2)	*T*12b2	– O42a	1.608(2)	152.4(1)	*T*22b2	– O31a	1.726(2)	*T*21b2	– O32b	1.615(2)	137.3(1)
	– O42b	1.726(2)		– O11b2	1.624(2)	138.6(1)		– O11b1	1.743(2)		– O12b2	1.626(2)	133.9(1)
	– O62a	1.732(2)		– O21b2	1.631(1)	138.3(1)		– O21b1	1.745(2)		– O52b	1.628(2)	146.0(1)
	– O12b2	1.740(2)		– O62b	1.634(1)	137.3(1)		– O52b	1.748(2)		– O22b1	1.631(2)	142.9(1)
Mean		1.731			1.624	141.7			1.741			1.625	140.0

distorted to space-group $P2_1/m$, causing an elliptical elongation of the *kgu* channel along [001] (Fig. 4a). Because of the random (Al,Si) distribution at the *T*-sites the mirror planes at $y = \frac{1}{4},\frac{3}{4}$ are still present (Fig. 5a), consequently establishing two enantiomorphic sheets of *T*-sites parallel (010) at $y \pm 0,\frac{1}{2}$ (Fig. 4a).

The most significant change in the framework of flörkeite is the (Al,Si) ordering at the *T*-sites. The mean Al–O and Si–O distances of the 16 *T*-sites are in the range from 1.731–1.743 Å to 1.615–1.631 Å, respectively, proving an ordered arrangement of the eight AlO_4- and eight SiO_4-tetrahedra (Table 5). The mean *T*–O–*T* angles vary from 138.6° to 144.4° (Table 5), values, which are well in the range of PHI-type compounds (Fischer & Baur, 2006). As a consequence of this (Al,Si) ordering, *i.e.* the loss of the mirror planes at $y = \frac{1}{4},\frac{3}{4}$ (Fig. 5b), and the pseudo-monoclinic distortion of the framework, the topochemical symmetry (Gottardi, 1979) of flörkeite is reduced to *B*2/*b*. Therefore, two slightly different sheets of *T*-sites occur at $y \pm 0,\frac{1}{2}$ (Fig. 4b and c) with a stronger elliptical elongation of the *kgu* 8^2-ring at $y \pm 0$ (*T*21b1(Si)–*T*21b2(Si): 9.102 Å, *T*12b1(Si)–*T*12b2(Si): 7.102 Å) than at $y \pm \frac{1}{2}$ (*T*22a1 (Al)–*T*22a2(Al): 8.836 Å, *T*11a1(Al)–*T*11a2(Al): 7.376 Å). The triclinic cell metric of flörkeite additionally induces a minor

Table 6. Selected interatomic distances (Å) for the extra-framework cation sites in flörkeite, standard deviations in parentheses.

K1	– OW6	2.839(3)	Ca1	– OW3C	2.398(2)
	– O21a1	2.861(2)		– OW4B	2.451(2)
	– O41a	2.934(2)		– OW5A	2.451(2)
	– OW3D	2.938(4)		– O61b	2.482(1)
	– O31b	2.976(2)		– O51a	2.495(2)
	– O42b	3.065(2)		– OW7	2.562(2)
	– O22b2	3.073(2)		– O21a2	2.564(2)
	– OW3B	3.077(2)		– OW2	2.729(2)
	[– O22a2	3.290(2)]			
	[– O32a]	3.737(2)]			
	[– O21b1	3.756(2)]			
K2	– O41b	2.769(2)	Ca2	– OW5B	2.378(2)
	– OW1	2.891(2)		– O12b1	2.398(2)
	– O21a2	2.933(2)		– OW1	2.412(2)
	– O22b1	3.015(2)		– OW3B	2.435(2)
	– OW2	3.015(3)		– O21b2	2.441(1)
	– O42a	3.030(2)		– OW4A	2.464(2)
	– OW3A	3.220(2)		– O62b	2.712(2)
	– O31b	3.351(2)			
	– OW3C	3.425(2)			
	[– O22a1	3.429(2)]			
	[– O21b2	3.654(2)]			
	[– O32b	3.940(2)]			
K3	– OW6	2.692(3)	Na1	– OW7	2.435(2)
	– OW4A	2.778(2)		– OW4B	2.454(2)
	– O11b1	2.944(2)		– O12b2	2.469(2)
	– O12a2	2.945(2)		– O21b1	2.475(2)
	– O61a	3.043(2)		– OW3A	2.504(2)
	– O31a	3.052(2)		– OW5B	2.536(2)
	– O62a	3.181(2)			
	[– O21a1	3.426(2)]			
	[– O22b2	4.033(2)]			
	[– O32a	5.075(2)]			

For the K-sites the three longest distances to the framework oxygen atoms of the 8-rings are given in square brackets.

Table 7. Closest O–O distances (Å) for the extra-framework H_2O-molecule sites in flörkeite, standard deviations in parentheses.

OW1	– O32a	2.801(2)	OW2	– OW4B	2.950(3)
	– O22a1	2.871(2)		– O61b	2.957(3)
	– OW4A	3.004(3)		– O11b2	3.007(3)
	– O12b1	3.072(2)		– O12a1	3.090(3)
OW3A	– OW3C	2.777(3)	OW3B	– O11b1	2.846(2)
	– O22b1	2.879(2)		– O42b	3.106(2)
	– O11b2	2.883(2)		– OW4A	3.107(2)
OW3C	– OW3A	2.777(3)	OW3B	– OW4A	2.857(4)
	– O12a1	2.840(3)		– OW5A	2.876(4)
	– OW7	2.852(3)		– O11a2	3.137(5)
OW4A	– OW3D	2.857(4)	OW4B	– O52b	2.708(2)
	– O51b	2.859(3)		– O62b	2.899(2)
	– OW1	3.004(3)		– OW2	2.950(2)
OW5A	– O61a	2.756(2)	OW5B	– O62a	2.737(2)
	– OW3D	2.876(4)		– O52a	2.757(2)
	– O61b	2.979(2)		– O21b2	2.936(2)
OW6	– O41a	2.933(3)	OW7	– O22a2	2.704(2)
	– O32b	3.011(3)		– OW3C	2.852(3)
				– OW4B	2.970(2)

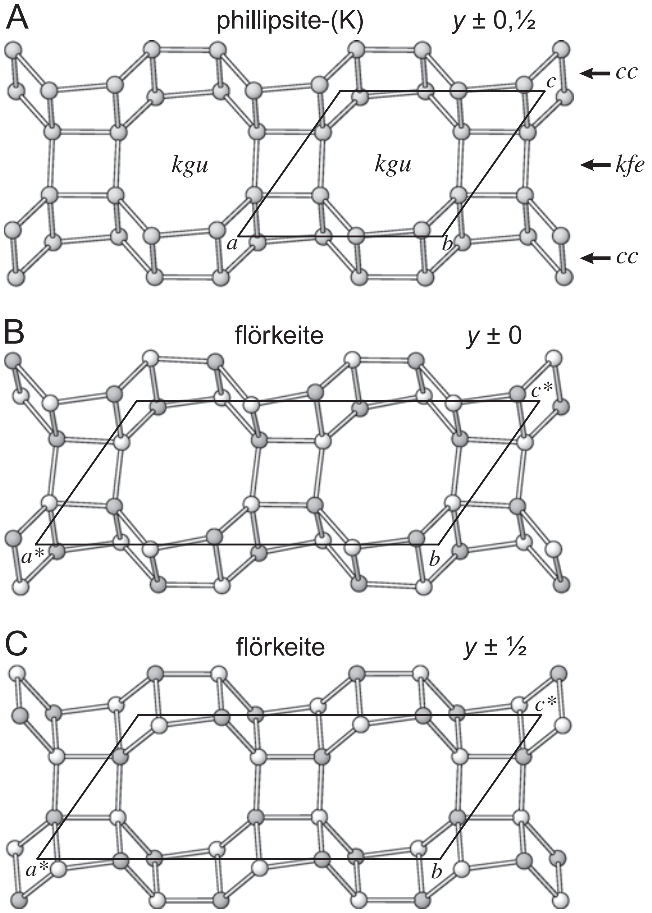

Fig. 4. View of the *T*-site sheets parallel (010) connecting the *kfe* channels of the frameworks at $y \pm 0,\frac{1}{2}$ of phillipsite-(K) (Rinaldi *et al.*, 1974) and flörkeite. The double crankshaft chain (*cc*) and the *kfe* channel along [100] are indicated by an arrow, the *kgu* channels are normal to the projection plane. For flörkeite, Al atoms are dark and Si atoms are light gray.

elliptical distortion along [0$\bar{2}$1] of the *kfe* 8^2-rings in the [100] channel system, and an increased tilt of the Al–Si connections (at $y \pm \frac{1}{2}$) between neighbouring *cc* chains (Fig. 5b). Comparing the structures of phillipsite-(K) and flörkeite, it is obvious that only small differences in the positions of the framework atoms exist. As can be seen from the data given in Table 4 the calculated distances between the corresponding *T*-sites and oxygen atoms of both frameworks are in the range from 0.039–0.250 Å to 0.018–0.483 Å, respectively. Furthermore, the crystal-chemical characteristic of the flörkeite framework reveals no indication for the observed doubling of the *a* parameter, which arises from the placement of extra-framework constituents solely. Although the observed ordering at the *T*-sites is not known for any natural occurrence of phillipsite, an equivalent ordering was reported for the Co-substituted tecto-aluminophosphates ACP-PHI (Feng *et al.*, 1997) and DAF-8 (Barrett *et al.*, 2006), both pseudo-orthorhombic with space-group *C*2/*c* and *Cc*, respectively.

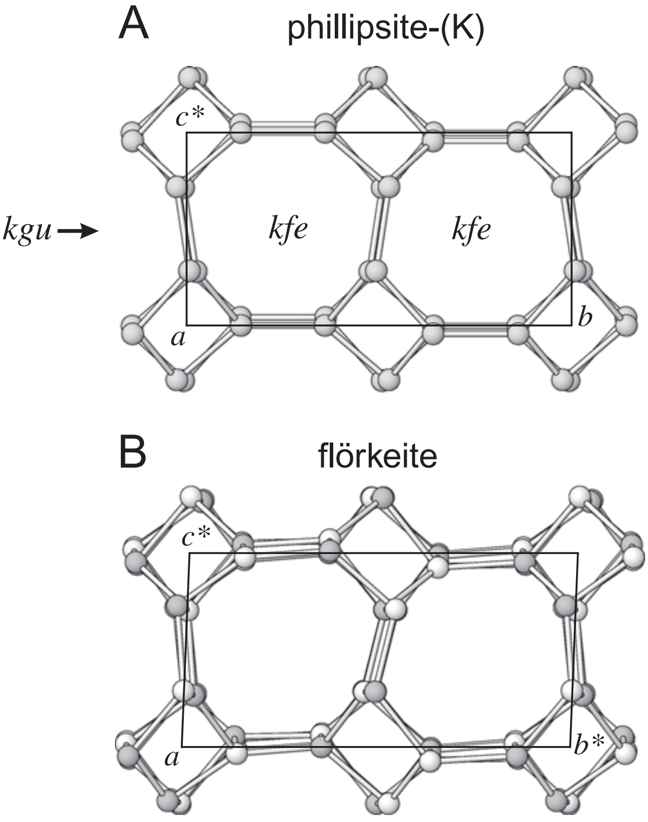

Fig. 5. View of the *T*-site arrangements of phillipsite-(K) (Rinaldi *et al.*, 1974) and flörkeite along [100]. The *kgu* channel along [010] is indicated by an arrow, the *kfe* channels are normal to the projection plane. For flörkeite, Al atoms are dark and Si atoms are light gray.

6.2. Extra-framework constituents

The extra-framework constituents of flörkeite are distributed over six cations (3 K, 2 Ca, 1 Na) and 12 OW-sites for the H_2O molecules (Table 4). The single-crystal data refinement revealed no short cation–cation or H_2O–H_2O contacts (Table 7) and, with exception of the K3 position, for all sites a full occupancy. Moreover, the values of the displacement parameters gave no indication for split positions within the system of units in flörkeite. The filling of the channel systems is defined by six interconnected cation–H_2O clusters ($K1(H_2O)_3$, $K2(H_2O)_4$, $K3(H_2O)_2$, $Ca1(H_2O)_5$, $Ca2(H_2O)_4$, $Na1(H_2O)_4$) allocated within the *oto* and *phi* units and bonded to the framework *via* cation–oxygen interactions (Table 6, Fig. 6). It is a distinct structural feature for flörkeite that all K^+ cations are located near the centre of the elliptically deformed 8-rings of the *oto* units, thus establishing a 5[+3] bonding scheme towards the framework oxygen atoms. The Ca^{2+} and Na^+ cations, on the other hand, are concentrated to the inner void of the *phi* units (Fig. 6).

K1 and K2 are located near the centre of the *oto* 8^1-ring. One H_2O ligand of $K1(H_2O)_3$ is in the centre of the *oto* unit (OW6), whereas the equivalent position beside

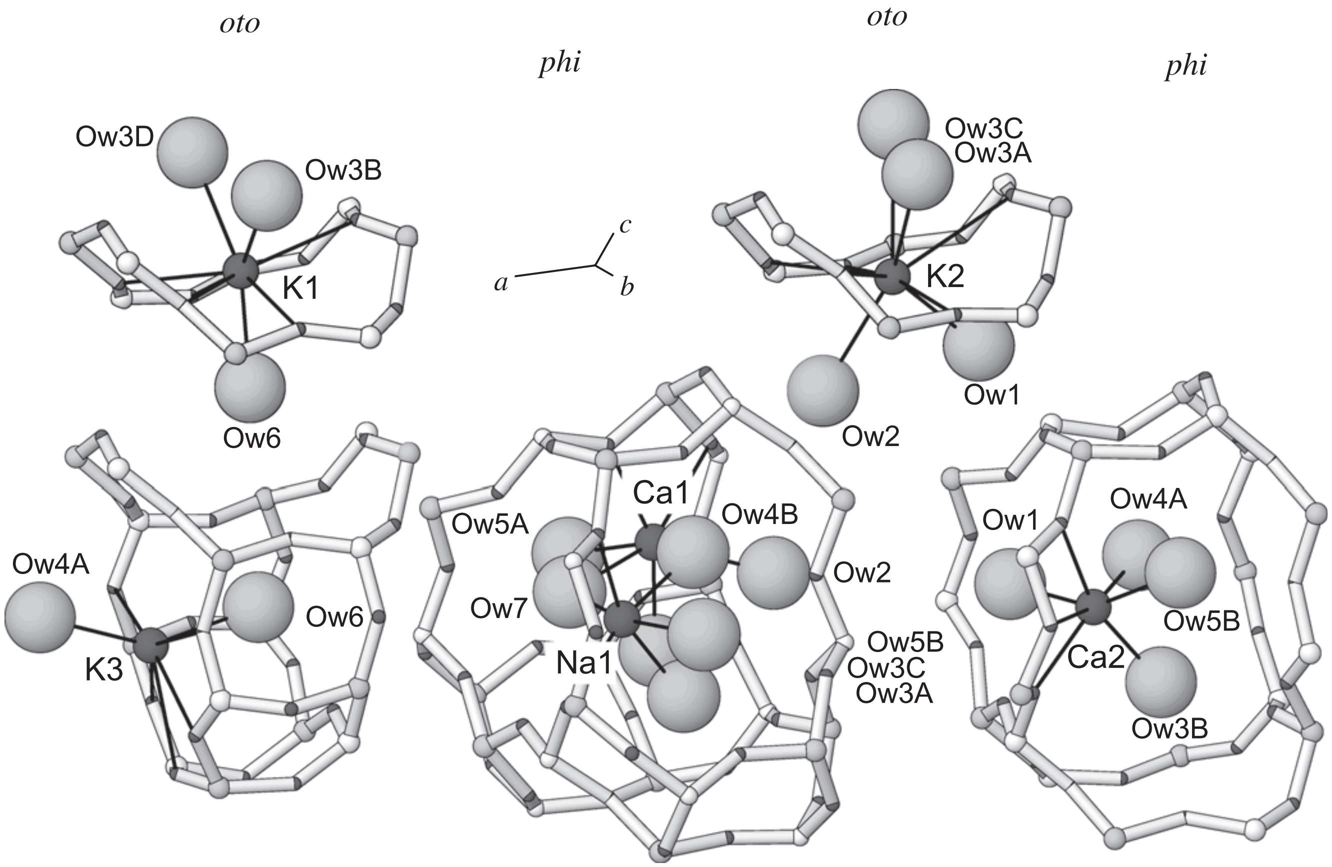

Fig. 6. Separated view of the *oto* and *phi* units of flörkeite to show the extra-framework arrangement of the K^+, Ca^{2+} and Na^+ cations (dark gray) bonded (black line) to the framework (O small black, Al dark gray, Si light gray) and the H_2O molecules (large gray spheres).

$K2(H_2O)_4$ is empty. Instead, a bonding scheme towards OW1 and OW2 in the adjacent *phi* units is established. These K positions were also reported by Rinaldi *et al.* (1974) to be the K site in phillipsite-(K) (Table 4). The $K3(H_2O)_2$ arrangement is located in the centre of an *oto* 8^2-ring, again bonded to 5 framework oxygen atoms and connected to $K1(H_2O)_3$ via OW6 (Fig. 6). This is different to the structure of phillipsite-(K), in which this site is occupied by H_2O (Table 4). The $Ca1(H_2O)_5$ and $Na1(H_2O)_4$ clusters are located together in the *phi* unit, thus building up a well-established H_2O bonding scheme. Both extra-framework sites are different to those in phillipsite-(K), in which Na1 is the Ca site and Ca1 is roughly equivalent to a H_2O position. The $Ca2(H_2O)_4$ inside the second, crystallographically different *phi* unit, however, is almost identical ($\Delta = 0.07$ Å) to the Ca position of phillipsite-(K).

As pointed out before, the main extra-framework characteristic of flörkeite is the doubling of the *a* parameter, which is induced by an ordering of the cations and H_2O molecules in the *kfe* channel system. Basically responsible for this ordering are alternating sequences of atom pairs with non-equivalent scattering factors along [100] and $\Delta \sim a/2$ (Fig. 7): Ca1–□–Ca1, Ca2–Na1–Ca2 and K3–OW2–K3. A minor contribution to the ordering arises also from the OW6–□–OW6 sequence in the centre of the *kfe* channel. In contrast, K1 and K2 and their bonded ligands OW3B, OW3D and OW3A, OW3C, respectively, follow a phillipsite-type ordering with *a*/2 (Fig. 6).

7. Classification and conclusion

As described above, flörkeite clearly represents the triclinically distorted, (Al,Si)-ordered analogue of phillipsite, with a $P2_1/m$ to $B2/b$ symmetry reduction of the framework topochemistry. Therefore, the topological density is identical for flörkeite and phillipsite (TD10 = 750.5), and the coordination sequences (Brunner & Laves, 1971) for the *T*-atoms of the flörkeite structure were proven (Bialek, 1995) to be identical with the two topologically distinct *T*-sites given for the PHI aristotype by Baerlocher *et al.* (2007); *T*1* : 4–9–18–32–50–71–94–122–157–195, *T*2*: 4–9–18–32–48–68–96–126–155–191. The framework density (Brunner & Meier, 1989) can be calculated to be 15.75, which is well within the range of PHI-type compounds (Fischer & Baur, 2006: 15.66–16.39). Following their given symmetry relationships within the Bärnighausen

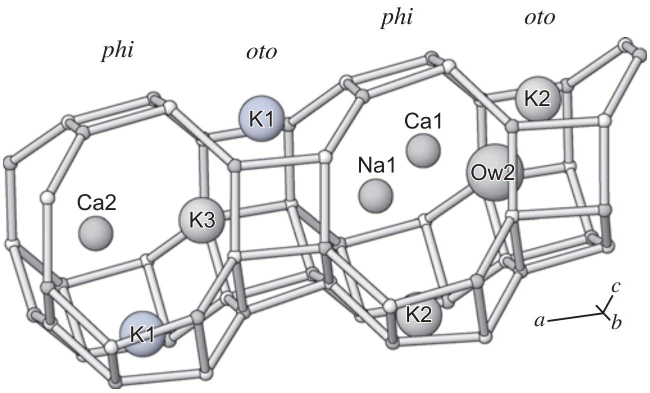

Fig. 7. The ordering along [100] of the extra-framework consitituents of flörkeite in the *oto* and *phi* units of the *kfe* channel at y±¾. Basically responsible for the doubling of the *a*-parameter are the non-equivalent pairs with $\Delta \sim a/2$: Cal-□, Ca2-Nal and K3-OW2. The equivalent pair K1-K2 follows a phillipsite type ordering with *a*/2. The oxygen atoms of the framework and the remaining H_2O molecules are omitted for clarity.

tree (Bärnighausen, 1980), flörkeite represents the VIII.2 subtype of the known PHI-type materials. Due to the elliptical elongation of the *kfe* and *oto* 8-rings the effective pore diameters, excluding the space within the Van-der-Waals radius for O of 1.5 Å, along [100] and [010] are 4.05 × 3.21 Å and 5.84 × 3.03 Å, respectively, which are slightly larger than the corresponding dimensions in phillipsite-(K) (Baerlocher *et al.*, 2007). According to the recommendations given by Coombs *et al.* (1998) flörkeite can be classified as the triclinically distorted, cation-ordered homomorph of phillipsite. Due to this zeolite naming convention, flörkeite-(K) can be used as a more distinguished name extension. The chemical name can be given as tripotassium dicalcium monosodium tecto-octoalumooctosilicate dodecahydrate.

Among the special extra-framework sites of zeolite-type compounds the centre of 8-rings is known to be a favoured site for the emplacement of large cations (*e.g.*, Fischer *et al.*, 2008). Therefore, the 8^1- and 8^2-rings of the *oto* unit play an important role in the structural implication of the K content on PHI-type compounds. Whereas K in the 8^1-ring is known for phillipsite-(K), K in the 8^2-ring is unique for flörkeite, which gives rise to the prediction that this position is the second favoured K position in PHI-type structures. And as the observed doubling of the *a* parameter in flörkeite is solely controlled by the ordering of the extra-framework constituents, a high-K chemical composition of phillipsite with ~3 K *pfu* will be the most promising candidate to exhibit a similar structural feature. A phillipsite chemistry with an almost even K content (~ 2 or ~ 4 K *pfu*), on the other hand, should induce phillipsite-type unit-cell dimensions. As a further inference, one can state that a high K content in the crystallization environment is the predominant controlling variable during the formation of flörkeite and high-K batches will be required for possible syntheses routes of flörkeite-type tecto-alumosilicates. Additionally, the observed (Al,Si) ordering can be attributed to the unusual, low-thermal conditions of formation within the Ca-rich xenolithic host, as it is also indicated by the co-occurence of the (Al,Si)-ordered zeolites willhendersonite, bellbergite and tschörtnerite.

Acknowledgements: The authors thank B. Ternes (Mayen – Hausen, Germany) for providing the material studied in the present paper, G. Blass (Eschweiler, Germany) for preliminary PXRD and SEM-EDS studies, M. Wagner for sample preparations as well as T. Ntaflos, M.A. Götzinger and G. Giester (all Wien, Austria) for their support with the chemical microanalyses and single-crystal X-ray diffraction. The useful comments of CNMNC members and an anonymous reviewer as well as the constructive contributions of R.X. Fischer (Bremen, Germany) are gratefully acknowledged. The work was supported by of the International Centre for Diffraction Data through Grant 90–03.

References

Abraham, K., Gebert, W., Medenbach, O., Schreyer, W., Hentschel, G. (1983): Eifelite, $KNa_3Mg_4Si_{12}O_{30}$, a new mineral of the osumilite group with octahedral sodium. *Contrib. Mineral. Petrol.*, **82**, 252–258.

Aiello, R. & Barrer, R.M. (1970): Hydrothermal chemistry of silicates. Part XIV. Zeolite crystallization in presence of mixed bases. *J. Chem. Soc. A*, **1979**, 1470–1475.

Baerlocher, Ch., McCusker L.B., Olson, D.H. (2007): Atlas of zeolite framework types, 6th Ed. Elsevier Science B.V., Amsterdam, 404 p.

Barrett, P.A., Sankar, G., Stephenson, R., Catlow, C.R.A., Thomas, J.M., Jones, R.H., Teat, S.J. (2006): A new addition to the phillipsite family of molecular sieves: A divalent metal-ion-framework substituted microporous aluminophosphate (DAF-8). *Solid State Sci.*, **8**, 337–341.

Bartelmehs, K.L., Bloss, F.D., Downs, R.T., Birch, J.B. (1992): EXCALIBR II. *Z. Kristallogr.*, **199**, 185–196.

Bärnighausen, H. (1980): Group-subgroup relations between space groups: a useful tool in crystal chemistry. *MATCH Commun. Math. Comp. Chem.*, **9**, 139–175.

Baur, W.H. & Fischer, R.X. (2000): ZSC.1, Zeolite structure and topology. *in* ''Microporous and other framework materials with zeolite-type structures'', W.H. Baur & R.X. Fischer, eds. Landolt Börnstein New Series IV/14/B, Springer Verlag, Berlin, 8–9.

Bialek, R. (1995): KRIBER1.1, Kristallographische Berechnungen. ETH Zürich, Zürich.

Bogaard, P. & Schmincke, H.-U. (1990): Die Entwicklungsgeschichte des Mittelrheinraumes und die Eruptionsgeschichte des Osteifel-Vulkanfeldes. *in* '''Rheingeschichte zwischen Mosel und Maas'', W. Schirmer, ed. Deuqua Führer, Hannover, **1**, 166–190.

Brunner, G.O. & Laves, F. (1971): Zum Problem der Koordinationszahl. *Wiss. Z. Tech. Univ. Dresden*, **20**(2), 387–390.

Brunner, G.O. & Meier, W.M. (1989): Framework density distribution of zeolite-type tetrahedral nets. *Nature*, **337**, 146–147.

Coombs, D.S., Alberti, A., Armbruster, T., Artioli, G., Colella, C., Galli, E., Grice, J.D., Liebeau, F., Mandarino, J.A., Minato, H., Nickel, E.H., Passaglia, E., Peacor, D.R., Quartieri, S., Rinaldi, R., Ross, M., Sheppard, R.A., Tillmanns, E., Vezzalini, G. (1998): Recommended nomenclature for zeolite minerals: Report of the Subcommittee on Zeolites of the International Mineralogical Association, Commission on New Minerals and Mineral Names. *Eur. J. Mineral.*, **10**, 1037–1081.

Davis, R.J. (1958): Mordenite, ptilolite, flokite, and arduinite. *Mineral. Mag.*, **31**, 887–888.

Doelter, C. (1921): Phillipsit. *in* ''Handbuch der Mineralchemie'', C. Doelter, ed. Steinkopff Verlag, Dresden, 138–150.

Effenberger, H., Giester, G., Krause, W., Bernhardt, H.-J. (1998): Tschörtnerite, a copper-bearing zeolite from the Bellerberg volcano, Eifel, Germany. *Am. Mineral.*, **83**, 607–617.

Feng, P., Bu, X., Stucky, G.D. (1997): Hydrothermal syntheses and structural characterization of zeolite analogue compounds based on cobalt phosphate. *Nature*, **388**, 735–741.

Fischer, R.X. & Baur, W.H. (2006): Zeolite-type crystal structures and their chemistry. Framework type code PHI. *in* ''Microporous and other framework materials with zeolite-type structures'', R.X. Fischer & W.H. Baur, eds. Landolt Börnstein New Series IV/14/D, Springer Verlag, Berlin, 412–425.

Fischer, R.X. & Tillmanns, E. (1988): The equivalent isotropic displacement factor. *Acta Crystallogr.*, **C44**, 775–776.

Fischer, R.X., Lengauer, C.L., Tillmanns, E., Ensink, R.J., Reiss, C.A., Fantner, E.J. (1993): PC-Rietveld plus, a comprehensive Rietveld analysis package for PC. *Mater. Sci. Forum*, **133–136**, 287–292.

Fischer, R.X., Kahlenberg, V., Lengauer, C.L., Tillmanns, E. (2008): Thermal behavior and structural transformation in the chabazite-type zeolite willhendersonite, $KCaAl_3Si_3O_{12}\cdot 5H_2O$. *Am. Mineral.*, **93**, 1317–1325.

Flörke, O.W. (1967): Die Modifikationen von SiO_2. *Fortschr. Mineral.*, **44**(2), 181–230.

Flörke, O.W., Flörke, U., Giese, U. (1984): Moganite. A new microcrystalline Silica-Mineral. *N. Jb. Mineral. Abh.*, **149**, 325–336.

Fresenius, W. (1879): Ueber den Phillipsit und seine Beziehungen zum Harmotom und Desmin. *Z. Krystallogr.*, **3**, 42–72.

Galli, E. & Loschi Ghittoni, A.G. (1972): The crystal chemistry of phillipsites. *Am. Mineral.*, **57**, 1125–1145.

Gandolfi, G. (1964): Metodo per ottenere uno spettro di polveri da un cristallo singolo di piccole dimensioni (fino a 30 μ). *Mineral. Petrogr. Acta*, **10**, 149–156.

Gottardi, G. (1979): Topologic symmetry and real symmetry in framework silicates. *Tschermaks Mineral. Petrogr. Mitt.*, **26**, 39–50.

Gottardi, G. & Galli, E. (1985): Natural zeolites. Springer Verlag, Berlin, 409 p.

Hentschel, G. & Kuzel, H.J. (1976): Strätlingit, $2CaO\cdot Al_2O_3\cdot SiO_2\cdot 8H_2O$, ein neues Mineral. *N. Jb. Mineral. Mh.*, **1976**, 326–330.

Hentschel, G. (1987): Die Mineralien der Eifelvulkane. 2nd Ed., Weise Verlag, München, 177 p.

Kolitsch, U. & Blass, G. (2005): Triclinic 'phillipsite' in a Ca-rich xenolith from the Bellerberg, Eifel, Germany: reduction of symmetry due to nearly complete Al–Si ordering – evidence for an unusual cooling history? *Mitt. Österr. Mineral. Ges.*, **151**, 66.

Lehmann, J. (1874): Über den Ettringit, ein neues Mineral, in Kalkeinschlüssen der Lava von Ettringen (Laacher Gebiet). *N. Jb. Mineral. Geol. Paläont.*, **1874**, 273–275.

Mandarino, J.A. (1981): The Gladstone-Dale relationship: Part IV. The compatibility concept and its application. *Can. Mineral.*, **19**, 441–450.

Meyer, W. (1994): Geologie der Eifel. 3rd Ed., Schweizerbart'sche Verlagsbuchhandlung, Stuttgart, 618 p.

Mihajlović, T., Lengauer, C.L., Ntaflos, T., Kolitsch, U., Tillmanns, E. (2004): Two new minerals, rondorfite, $Ca_8Mg[SiO_4]_4Cl_2$, and almarudite, $K(\square, Na)_2(Mn,Fe,Mg)_2(Be,Al)_3[Si_{12}O_{30}]$, and a study on iron-rich wadalite, $Ca_{12}[(Al_8Si_4Fe_2)O_{32}]Cl_6$, from the Bellerberg (Bellberg) volcano, Eifel, Germany. *N. Jb. Mineral. Abh.*, **179**, 265–294.

Otwinowski, Z. & Minor, W. (1997): Processing of X-ray diffraction data collected in oscillation mode. *Meth. Enzymol.*, **276**, 307–326.

Otwinowski, Z., Borek, D., Majewski, W., Minor, W. (2003): Multiparametric scaling of diffraction intensities. *Acta Crystallogr.*, **A59**, 228–234.

Rinaldi, R., Pluth, J.J., Smith, J.V. (1974): Zeolites of the phillipsite family. Refinement of the crystal structures of phillipsite and harmotome. *Acta Crystallogr.*, **B30**, 2426–2433.

Rüdinger, B., Tillmanns, E., Hentschel, G. (1993): Bellbergite – a new mineral with the zeolite structure type EAB. *Mineral. Petrol.*, **48**, 147–152.

Sheldrick, G.M. (1997a): SHELXS-97, a program for the solution of crystal structures. Universität Göttingen, Göttingen.

— (1997b): SHELXL-97, a program for crystal structure refinement. Universität Göttingen, Göttingen.

Smith J.V. (2000): Tetrahedral frameworks of zeolites, clathrates, and related materials. *in* ''Microporous and other framework materials with zeolite-type structures'', W.H. Baur & R.X. Fischer, eds. Landolt Börnstein New Series IV/14/A, Springer Verlag, Berlin, 266 p.

Straumanis, M. & Jevinš, A. (1936): Präzisionsaufnahmen nach dem Verfahren von Debye und Scherrer. II. *Z. Physik*, **98**, 461–475.

Tillmanns, E., Fischer, R.X., Baur, W.H. (1984): Chabazite-type framework in the new zeolite willhendersonite, $KCa[Al_3Si_3O_{12}]\cdot 5H_2O$. *N. Jb. Mineral. Mh.*, **1984**, 547–558.

Tschernich, R.W. (1992): Zeolites of the world. Geoscience Press, Phoenix, 563 p.

Wilson, A.J.C. & Prince, E. (1999): International tables for crystallography, Vol C: mathematical, physical and chemical tables. 2nd Ed., Kluwer, Dordrecht, 992 p.

Received 9 January 2009
Modified version received 1 March 2009
Accepted 14 April 2009